

Indication of a Hydrogen-Atom Abstraction Reaction Relevant to a Mechanistic Proposal for the Oxygen-Evolving Complex of Photosystem II

Kenneth Bendix Jensen, Christine J. McKenzie,* and Jens Zacho Pedersen

Chemistry Institute, University of Southern Denmark, Odense, 5230 Odense M, Denmark

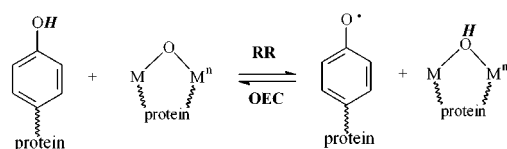
Received May 7, 2001

Hydrogen atom abstraction processes involving noncoordinated tyrosine residues are proposed as mechanistically important for some metalloenzymes. In the R2 unit of ribonucleotide reductase (RR), a diiron oxide species, compound X (probably a $\{\text{Fe}^{\text{III}}-(\mu\text{-O})_2\text{Fe}^{\text{IV}}\}$ core structure), abstracts a hydrogen atom from the nearby tyrosine Y_{122} to initialize the radical transfer pathway ultimately responsible reduction of the sugar unit of ribonucleotides.¹ An analogous reaction, but in the reverse direction, has been suggested for the conversion of water to dioxygen at the oxygen-evolving complex (OEC) of photosystem II; the tyrosine radical Y_z^* abstracts a hydrogen atom from a coordinated hydroxide with concomitant oxidation of a manganese ion.^{2,3} These reactions can be illustrated by Scheme 1. The reaction proceeding left to right shows the scenario for RR where $\text{M} = \text{Fe}$; from right to left the scenario for OEC where $\text{M} = \text{Mn}$.

Elucidation of H-atom abstraction processes in biological systems is aided by the study of analogous processes in simpler compounds. Mayer and co-workers have carried out pioneering studies in prediction of the H-atom abstraction energetics in the oxidation of hydrocarbon substrates by metal-oxo and metal coordination complexes.^{4,5} A system closely related to biological systems in terms of metal oxidation state is $[(\text{phen})_2\text{Mn}(\mu\text{-O})_2\text{Mn}(\text{phen})_2]^{3+}$, which is capable of oxidizing dihydroanthracene (DHA) to anthracene with resultant formation of $[(\text{phen})_2\text{Mn}(\mu\text{-OH})_2\text{Mn}(\text{phen})_2]^{3+}$.⁶ The reaction proceeds by two consecutive steps, both involving H-atom abstraction from the substrate coupled with concomitant protonation of the oxo bridge and one electron reduction of the metal center. Karlin and co-workers showed that $[(\text{MePY}_2)\text{Cu}(\text{O}_2)\text{Cu}(\text{MePY}_2)]^{2+}$ ($\text{MePY}_2 = N$ -methyl- N -bis[2-(2-pyridyl)ethyl]amine) can similarly effect H-atom abstraction from DHA.⁷ These processes are examples of the $\{\text{M}(\mu\text{-O})_2\text{M}\}$ core as an H-atom abstractor, and as such, they model to some extent (the organic reaction partners are not phenols) the left to right RR process in Scheme 1. Proposed here is the first example of a model for the reverse reaction in Scheme 1. A phenoxide radical and a μ -hydroxide bridged Cr–Mn complex have been used as reaction partners. Typically analogous μ -hydroxo dichromium complexes show $\text{p}K_{\text{a}}$ values many orders of magnitude higher than those for dimanganese complexes. The combination of Cr and Mn may have led to an appropriate homolytic bond dissociation energy (BDE_{OH}) for H-abstraction from a μ -OH group by a biologically relevant phenoxide radical.

The violet hydroxide-bridged Cr(III)–Mn(II) complex, $[(\text{Me}_3\text{tacn})\text{Cr}(\mu\text{-OH})(\mu\text{-CH}_3\text{CO}_2)_2\text{Mn}(\text{MeDPA})](\text{ClO}_4)_2$, **1**· $(\text{ClO}_4)_2$ ($\text{Me}_3\text{-tacn} = \text{tri-}N,N',N''\text{-methyltriazacyclononane}$, $\text{MeDPA} = N$ -methyl-

Scheme 1



N -bis(2-pyridylmethyl)amine), was prepared using Wieghardt and co-worker's method for the preparation of the oxo-bridged Cr(III)–Mn(III) complex, $[(\text{Me}_3\text{tacn})\text{Cr}(\mu\text{-O})(\mu\text{-CH}_3\text{CO}_2)_2\text{Mn}(\text{tacn})](\text{ClO}_4)_2$, **2**, ($\text{tacn} = \text{tri-}N,N',N''\text{-methyltriazacyclononane}$),⁸ with the exception that tacn was replaced by MeDPA .⁹ The spontaneous reduction of the starting Mn(III) ions to give the Mn(II) ion of the product, and the presence of a μ -hydroxide group in **1**, is in contrast with the combination of a Mn(III) ion and μ -oxide group found in **2**. MeDPA is a weaker-field ligand than tacn , and this is presumably the reason for the contrasting products in the analogous syntheses of **1** and **2**. The synthetic outcome prompted our investigation into H-atom abstraction from complex **1**.

To model as closely as possible the situation in OEC, the tyrosine-like 2,4,6-triphenylphenoxide radical (TPP^*)¹⁰ was used as an H-atom abstractor. TPP^* is generated in situ from the 2,4,6-triphenylphenoxyl dimer (TPPD) in the course of the following reaction: complex **1** and TPPD are mixed in stoichiometric proportions (2:1, respectively) in nitromethane or acetonitrile.¹¹ An intense maroon color forms instantaneously due to formation of the oxo-bridged Cr(III)–Mn(III) cation, **3** (Scheme 2). The UV–visible spectra of **1**¹² and the H-abstracted product, **3**,¹¹ in acetonitrile are very similar to those reported for $[(\text{tacn})\text{Cr}(\mu\text{-OH})(\mu\text{-CH}_3\text{CO}_2)_2\text{Mn}(\text{tacn})](\text{ClO}_4)_2$ ¹³ and **2**,⁸ respectively.

Comparisons of m/z values and gas-phase fragmentation patterns in mass spectrometric experiments were used in the characterization of **1** and **3**. The ESI mass spectrum¹⁴ of **1**· $(\text{ClO}_4)_2$, Figure 1(a), shows the doubly charged **1** as the major cation at an m/z of 313.1. Substantial fragmentation of this ion to mononuclear Cr- and Mn-containing ions occurred unless the potential difference between the nozzle and the skimmer was kept small. The daughter ions, $[(\text{MeDPA})\text{Mn}(\text{CH}_3\text{CO}_2)]^+$ and $[(\text{Me}_3-$

- (1) Waller, B. J.; Lipscomb, J. D. *Chem. Rev.* **1996**, *96*, 2625–2657.
- (2) Hoganson, C. W.; Babcock, G. T. *Science* **1997**, *277*, 1953–1956.
- (3) Yachandra, V. T.; Sauer, K.; Klein, M. P. *Chem. Rev.* **1996**, *96*, 2927–2950.
- (4) Mayer, J. M. *Acc. Chem. Res.* **1998**, *31*, 441–450.
- (5) Gardner, K. A.; Mayer, J. M. *Science* **1995**, *269*, 1849–1851.
- (6) Wang, K.; Mayer, J. M. *J. Am. Chem. Soc.* **1997**, *119*, 1470–1471.
- (7) Obias, H. V.; Lin, Y.; Murthy, N. N.; Pidcock, E.; Solomon, E. I.; Ralle, M.; Blackburn, N. J.; Neuhold, Y.-M.; Zuberbüler, A. D.; Karlin, K. J. *Am. Chem. Soc.* **1998**, *120*, 12960–12961.

- (8) Hotzelmann, R.; Wieghardt, K.; Flörke, U.; Haupt, H.-J.; Weatherburn, D. C.; Bonvoisin, J.; Blondin, G.; Girerd, J.-J. *J. Am. Chem. Soc.* **1992**, *114*, 1681–1696.
- (9) Reaction of 2 equiv of $(\text{Me}_3\text{tacn})\text{CrBr}_3$ ⁹ with $\{[(\text{MeDPA})\text{Mn}(\text{CH}_3\text{CO}_2)_2\text{O}](\text{ClO}_4)_2\}$ ¹¹ in the presence of excess acetate ions in methanol gives **1** in a 54% yield. Complex **1** has been crystallographically characterized (Supporting Information).
- (10) Dimroth, K.; Kalk, F.; Sell, R.; Schlömer, K. *Justus Liebigs Ann. Chem.* **1959**, *624*, 51–79.
- (11) Complex **1** and 0.5 equiv of TPPD (Aldrich) mixed in acetonitrile in 10^{-3} – 10^{-4} M concentrations. UV–vis data for **3**: λ , nm (ϵ , $\text{M}^{-1}\text{cm}^{-1}$): 492 (580), 553 (590), 682 (190), 731 (210), 774 (200).
- (12) UV–vis: λ , nm (ϵ , $\text{M}^{-1}\text{cm}^{-1}$): 419 (106), 536 (82), 664 (7), 697 (5).
- (13) Chaudhuri, P.; Winter, M.; Küppers, H.-J.; Wieghardt, K.; Nuber, B.; Weiss, J. *Inorg. Chem.* **1987**, *26*, 3302–3310.
- (14) Recorded on a Finnigan TSQ 700MAT triple-quadrupole instrument equipped with a nano-electrospray source.

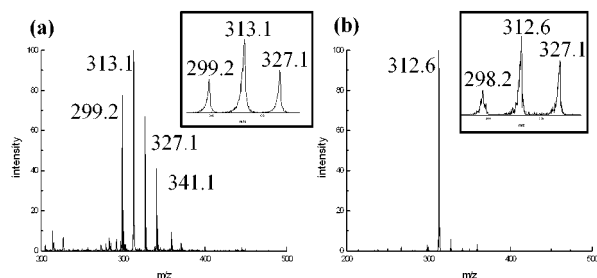


Figure 1. The ESI mass spectrum (a) of **1** and (b) of **3**, using identical source conditions. The insets show the main daughter ions after CID of the $m/z = 313.1$ ion of **1** and the $m/z = 312.6$ ion of **3**. Assignments, m/z : 313.1, **1**; 327.1, [(MeDPA)Mn(CH₃CO₂)⁺]; 341.1, [(Me₃tacn)Cr(CH₃CO₂)₂]⁺; 299.2, [(Me₃tacn)Cr(OH)(CH₃CO₂)⁺]; 312.6, **3**; 298.2, [(Me₃tacn)Cr(O)(CH₃CO₂)⁺].

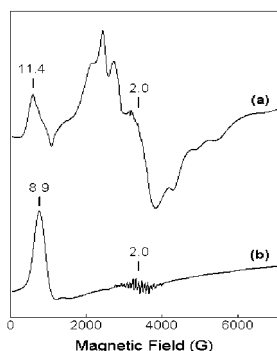
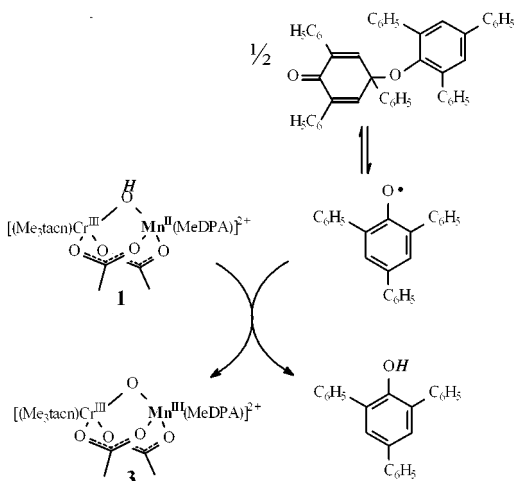


Figure 2. The ESR spectrum of (a) **1** in nitromethane and (b) **3** generated by addition of 0.5 molar equiv of TPPD to the solution in (a).¹⁷

Scheme 2



tacn)Cr(OH)(CH₃CO₂)⁺, were also generated from **1** in a separate collision induced dissociation (CID) experiment, shown as an inset in Figure 1(a). ESI mass spectra of the reaction mixture after addition of TPP⁺, recorded using the same source conditions, shows the doubly charged **3** with an m/z of 312.6 as the dominant peak, Figure 2(b). Thus, **3** is significantly more stable than **1** toward source fragmentation, reflecting a more strongly bonding μ -oxo group of **3** compared with the μ -hydroxo group of **1**. In a CID experiment (using higher energy collisions to those used for **1**), **3** fragments into [(Me₃tacn)Cr(O)(CH₃CO₂)⁺ and [(MeDPA)-Mn(CH₃CO₂)⁺ (inset Figure 2(b)). This indicates an internal disproportionation, Cr^{III}Mn^{III} → Cr^{IV} + Mn^{II}, with the oxo group staying with the Cr fragment. The match to the calculated isotopic distribution for **3** demonstrates that the reaction is very close to completion.¹⁵

The ESR spectrum¹⁶ of **1** in nitromethane, Figure 2(a), contains broad features consistent with the presence of the expected weakly antiferromagnetically coupled Cr(III) and Mn(II) ions. The singlet for the TPP⁺ is found at $g = 2.00561$ in the ESR spectrum of the TPPD in nitromethane. Figure 2(b) shows that when a solution of the phenoxide radical is mixed with a solution of **1** (stoichiometry, TPPD:**1** = 1:2), the organic radical signal disappears completely and the complex-derived signals simplify. The d⁴ Mn(III) of **3** is expected to be ESR silent, and the resultant signal ($g = 8.9$) is ascribed to the Cr(III) ion only.

The results described above verify the identities of **1** and **3**. That the reaction might be classified as an H-atom abstraction rather than proton coupled electron transfer is based on the following observations: the (i) cyclic voltammogram (CV) of **1**¹⁵ and (ii) acid/base titrations. The CV of **1** in acetonitrile shows two reversible redox waves rather close together at 447 and 630 mV above the Fc/Fc⁺ couple. If deprotonation spontaneously followed Mn oxidation, then a CV would be expected to show an irreversible oxidation. The first reversible oxidation wave implies a [Cr(III)-(μ-OH)-Mn(II)] ↔ [Cr(III)-(μ-OH)-Mn(III)] process, i.e., the bridging hydroxide remains intact after electrochemical oxidation, contrasting to the situation after radical oxidation. Titration of **1** with triethylamine or hydroxide did not result in the spectroscopic detection of **3**. Excess hydroxide led ultimately to the decomposition of **1**. Further, addition of 1 equiv of perchloric acid to solutions of **3** did not regenerate **1**, and excess perchloric acid led to the formation of pale yellow solutions without detection of **1**. These attempted deprotonation and protonation reactions of **1** and **3**, respectively, again suggest that redox-coupled acid-base chemistry is not operative.

Further analysis of the electrochemical behavior in various solvents, and measurement of the pK_a of **1**, is needed in order to estimate the BDE_{OH} for the μ-OH of complex **1**. Using this information, Pecoraro and co-workers have concluded that H-atom abstraction by a tyrosine radical from hydroxide bridged Mn(III)-Mn(IV) and Mn(III)-Mn(IV) dimers is thermodynamically feasible.¹⁸⁻²⁰ In conclusion, the present Cr-Mn system appears to model the H-atom abstraction step in mechanistic proposals^{2,3} for OEC. We have demonstrated that oxidation of the Mn(II) to Mn(III) is a consequence of oxidation by a phenoxide radical, and the evidence supports a H-atom abstraction mechanism. Cr is not biologically relevant; however, in addition to playing a probable role in tuning the BDE_{OH} and providing an ESR spectroscopic handle, the robust Cr(III) in **1** may be a key feature in preventing alternative reactions and rearrangements upon radical oxidation.

Acknowledgment. Professors James Mayer (University of Washington) and Hans Toftlund (University of Southern Denmark) are thanked for helpful discussions. Funding was provided by The Danish Natural Science research council (C.J.M.).

Supporting Information Available: Syntheses of {(MeDPA)Mn(CH₃CO₂)₂O}(ClO₄)₂ and **1**; drawing of X-ray structure of **1** and listings of bond lengths and angles; UV-visible spectra of **1** and **3**; CV of **1**; and expansions of mass spectra and calculated isotopic patterns. This material is available free of charge via the Internet at <http://pubs.acs.org>.

IC0155380

(15) Supporting Information.

(16) Recorded on a Bruker EMX113 at 100 K.

(17) The weak 16 line signal at $g = 2$ is due to a Mn(III)-Mn(IV) impurity originating from the oxo-bridged dimanganese compound used in the synthesis of **1**, trace amounts are also present in the spectrum of **1** in Figure 2(a).

(18) Pecoraro, V. L.; Baldwin, M. J.; Tyler Caudle, M.; Hsieh, W.-Y.; Law, N. A. *Pure Appl. Chem.* **1998**, *70*, 925-929.

(19) Baldwin, M. J.; Pecoraro, V. L. *J. Am. Chem. Soc.* **1996**, *118*, 11325-11326.

(20) Tyler Caudle, M.; Pecoraro, V. L. *J. Am. Chem. Soc.* **1997**, *119*, 3415-3416.